Optica Applicata, Vol. L, No. 3, 2020
DOI: 10.37190/oa200307

A diode-pumped high-repetition-frequency passively *Q*-switched Nd:$LaMgAl_{11}O_{19}$ laser

YAN XU, ZIYE GAO, GUANGQIONG XIA, ZHENGMAO WU*

School of Physical Science and Technology, Southwest University, Chongqing 400715, China

*Corresponding author: zmwu@swu.edu.cn

High-repetition-frequency *Q*-switched laser is realized through adopting a Nd:$LaMgAl_{11}O_{19}$ (Nd:LMA) disordered crystal as the gain material, a laser diode lasing at 796 nm as the pumped source, and a semiconductor saturable absorber mirror (SESAM) as the *Q*-switched device. The output characteristics are analyzed under using different transmittance *T* plane mirrors as an output coupler. Without adopting SESAM, the laser is operating at a CW state, and a relatively high transmittance is helpful for achieving high output power, slope efficiency and light-to-light efficiency. For $T = 7.5\%$ and an absorbed power of 6.17 W, the output power arrives at its maximum of 1160 mW, and the corresponding slope efficiency and light-to-light efficiency are 20.71% and 18.78%, respectively. After introducing SESAM into the cavity, the laser operates at a passively *Q*-switched state, and the largest slope efficiency is 13.14% under $T = 5.0\%$. Adopting five different output couplers, with the increase of the absorbed power, the pulse repetition frequencies, the pulse energies and the peak powers will ascend while the pulse widths will decline. The observed narrowest pulse width, the maximum pulse repetition frequency, the highest pulse energy and peak power are 1.745 μs, 175.88 kHz, 3.21 μJ and 1.84 W, respectively.

Keywords: Nd:$LaMgAl_{11}O_{19}$ disordered crystal, *Q*-switched laser, high pulse repetition frequency (PRF), semiconductor saturable absorber mirror (SESAM), laser diode (LD).

1. Introduction

Diode-pumped solid-state (DPSS) *Q*-switched lasers have attracted much attention in the fields of nonlinear optics, laser marking, medical diagnostics, material processing, photoacoustic imaging and remote sensing due to their unique advantages such as compactness, good beam quality, low cost and high pulse repetition frequency [1–5]. As is well-known, for achieving *Q*-switched laser, two main *Q*-switching methods are used: one is active *Q*-switching via additional modulators, and the other is passive *Q*-switching by introducing saturable absorbers into the laser cavity to control intracavity loss [6, 7]. Comparatively speaking, a passively *Q*-switched laser possesses more simple structure, which is beneficial for reducing the loss and improving the efficiency. Many devices such as a semiconductor saturable absorber mirror (SESAM) [8–10], Cr:YAG [11, 12], graphene [13] and WS_2 [14] can be taken as the saturable absorbers in the DPSS passively *Q*-switched lasers.

Neodymium-doped (Nd-doped) materials such as Nd:YAG, Nd:LuAG, Nd:$GdVO_4$, *etc*., have been widely used as the gain materials in DPSS passively *Q*-switched lasers owing to their advantages including long lifetime, relatively large emission cross-section and large thermal conductivity [15, 16]. Generally, a gain medium with high dopant concentration and long fluorescence lifetime is promising for achieving high power. However, limited by the concentration quenching and the cluster effect, the Nd^{3+}-doping concentration for many Nd-doped ordered crystals is relatively low, such as Nd^{3+}-doping concentration of 0.5 at.% in $GdVO_4$ [17], 1.0 at.% in YAG [18], 1.0 at.% in LuAG [19] and 1.0 at.% in YVO_4 [20]. For $LaMgAl_{11}O_{19}$ (LMA), as a disordered crystal, the Nd^{3+}-doping concentration can be improved to 10 at.% [21], and meanwhile its fluorescence lifetime is about 321 μs [22], which is larger than 156 μs for Nd:YPO_4 [23] and 100 μs for Nd:$GdVO_4$ [24]. As a result, Nd:LMA may be suitable to be the gain material in high power lasers, and then the performances of the laser based on Nd:LMA have attracted much attention [25, 26]. Lu *et al*. reported a continuous-wave (CW) laser based on Nd:LMA with Nd^{3+}-doping concentration of 3 at.%, and the output power is 30 mW [25]. Pan *et al*. demonstrated that the CW output power of a diode-pumped Nd:LMA laser, in which the Nd:LMA disordered crystal is grown by the Czochralski method, can reach a watt level [22]. Very recently, Wang *et al*. reported that, adopting a Cr:YAG saturable absorber as a *Q*-switched device, a DPSS passively *Q*-switched Nd:LMA laser can generate pulses at around 1054 nm with average watt-level output power, and the highest pulse repetition frequency (PRF) is 42.40 kHz [26].

In this work, adopting a SESAM as a passively *Q*-switched device, a DPSS high-repetition-frequency (>100.00 kHz) passively *Q*-switched Nd:LMA laser is demonstrated. During the experiment, a Nd:LMA disordered crystal with Nd^{3+}-doping concentration of 5 at.% and dimension of $3 \times 3 \times 5$ mm^3 is used as the gain medium and a laser diode lasing at 796 nm is used as the pump source. Through adopting five mirrors with different transmittances to be the output coupler, the output characteristics of the laser have been investigated in detail.

2. Experimental setup

The gain medium used in the experiment is an uncoated Nd:$LaMgAl_{11}O_{19}$ (Nd:LMA) disordered crystal [22]. It is successfully grown by the Czochralski method and cut along *c*-direction with Nd^{3+}-doping concentration of 5 at.% and dimension of 3×3×5 mm^3 (5 mm of the thickness). The maximum peak absorption cross-section of the Nd:LMA crystal is 1.7×10^{-20} cm^2 at 795 nm for σ polarization as shown in Ref. [22]. Therefore, a laser diode (LD) with an emission wavelength around 796 nm is used as a pump source, and it is coupled with a fiber whose core diameter is 105 μm and numerical aperture is 0.22. Its output is focused into the Nd:LMA crystal via a 1:1 coupling system. For effective thermal conduction, the Nd:LMA disordered crystal is wrapped by an indium foil, and it is mounted in a water-cooled copper heat sink whose temperature is stabilized at about 17°C. The absorption efficiency of the Nd:LMA disordered crystal is measured to be about 58.65%.

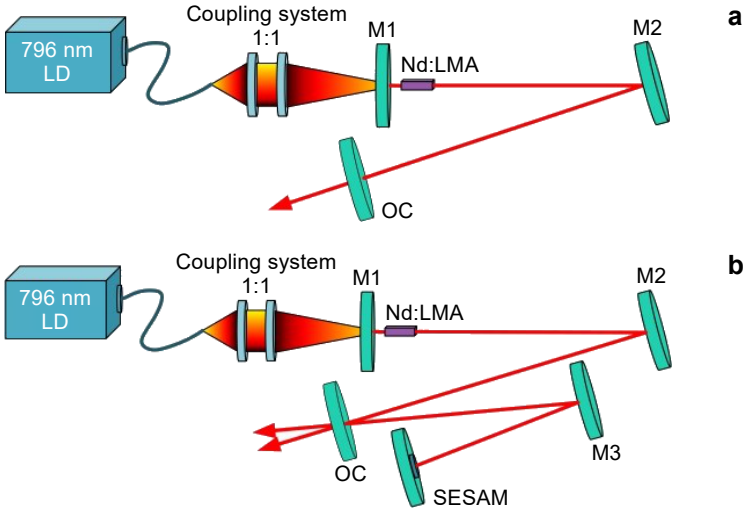

Fig. 1. Experimental setups for diode-pumped Nd:LMA lasers under CW operation (**a**) and passively *Q*-switching (**b**). LD: laser diode, M1: dichroic mirror, M2, M3: concave mirrors, OC: output coupler, and SESAM: semiconductor saturable absorber mirror.

The experimental setups for the diode-pumped Nd:LMA laser operating at continuous-wave (CW) state (**a**) and passively *Q*-switched state (**b**) are illustrated in Fig. 1. Under the CW state (as shown in Fig. 1**a**), the laser cavity is composed of a dichroic mirror (M1), a concave mirror (M2), and an output coupler (OC). M1 possesses high transmission at 796 ± 10 nm and high reflection at 1000–1100 nm, and M2 with a radius of curvature of 200 mm provides high reflectivity at 940–1100 nm. Five output couplers (named as OC1–OC5) are tried in the experiment, and their transmittances *T* are 0.5%, 1.6%, 2.5%, 5.0% and 7.5% at the lasing wavelength of 1056 nm, respectively. Under the passively *Q*-switched state (as shown in Fig. 1**b**), the laser cavity is composed of a dichroic mirror (M1), two concave mirrors (M2, M3), an output coupler (OC), and a semiconductor saturable absorber mirror (SESAM). Mirror M3 with a radius of curvature of 300 mm provides high reflectivity at 900–1100 nm. The SESAM (BATOP GmbH) operates at 1020–1110 nm, and it has a saturated absorption of 0.7%, a saturation fluence of about 120 μJ/cm^2 and a recovery time of 1 ps. The output of laser is analyzed in the optical domain and time domain via an optical spectrum analyzer (Ando AQ6317C, 600–1750 nm) and an oscilloscope (Agilent Technologies DS09254A), respectively. Optical powers are measured using an optical power meter (Thorlabs-PM100D, Thorlabs-CAL).

3. Experimental results and discussion

Without introducing a semiconductor saturable absorber mirror (SESAM) (shown in Fig. 1**a**), Nd:LaMgAl$_{11}$O$_{19}$ (Nd:LMA) laser is operating at a CW state. Figure 2**a** displays the dependence of the output power on the absorbed power. In the work, the ab-

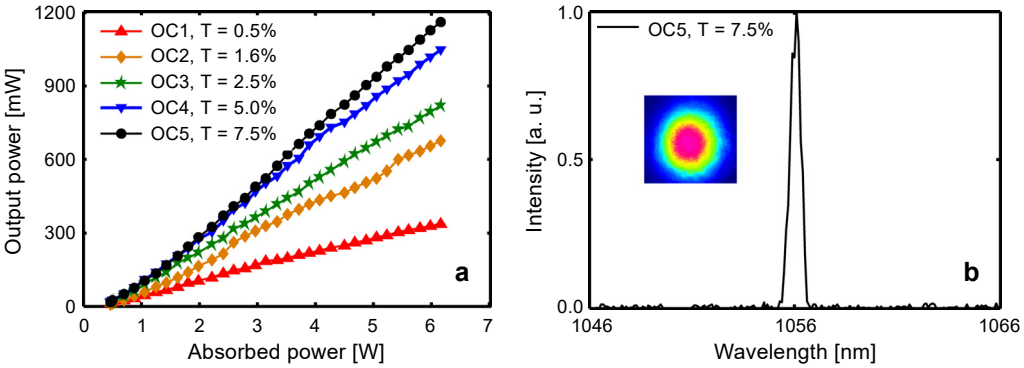

Fig. 2. Performances of the CW Nd:LMA laser. Dependence of the output power on the absorbed power for different OCs (**a**); optical spectrum for OC5 (T = 7.5%) under an absorbed power of 2.23 W (**b**).

sorbed power is characterized as follows: removing the Nd:LMA disordered crystal, we put the optical power meter at the location of the crystal to measure the power from the laser diode (LD), and the absorbed power is equal to the power value recorded by the power meter multiplied by the absorption efficiency of Nd:LMA (58.65%). During the experiment, the absorbed power can be adjusted through controlling the output power of the LD. To avoid damage to the Nd:LMA disordered crystal, the absorbed power is not more than 6.17 W during the experiment. From this diagram, it can be seen that, for the five output couplers (OCs), the threshold absorbed powers are all about 0.46 W. Once the absorbed powers exceed the threshold absorbed power, the output power linearly increases with the increase of the absorbed power. For the absorbed power increased to 6.17 W, under OC1–OC5, the maximum output powers arrive at 335, 672, 818, 1044, and 1160 mW, respectively, the corresponding light-to-light efficiencies are 5.43%, 10.88%, 13.25%, 16.91%, and 18.78%, and the slope efficiencies are 5.79%, 12.15%, 14.35%, 18.55%, and 20.71%, respectively. As a result, adopting an OC with a relatively high transmittance may be helpful for achieving a good performance output. Figure 2**b** shows the measured optical spectrum and spatial distribution for CW Nd:LMA laser under T = 7.5% and the absorbed power of 2.23 W. The central wavelength is about 1056 nm, and the spatial distribution of the beam measured by a CCD camera (Beam On, IR1550) indicates that the laser is operating at a fundamental mode.

In order to realize Q-switched operation, a concave mirror M2 and a SESAM are added into the system (as shown in Fig. 1**b**). Figure 3 measures the average output power as a function of the absorbed power for the Nd:LMA laser operating at a passively Q-switched state. Obviously, the absorbed power regions, in which the laser is operating at a stable Q-switched state, are different for different OCs employed, and they are 2.59–5.98 W, 2.59–5.61 W, 2.59–5.43 W, 2.59–4.68 W, and 2.78–5.98 W for OC1–OC5, respectively. With the increase of the absorbed power, the average output power will increase. The maximum average output power is 551 mW obtained under

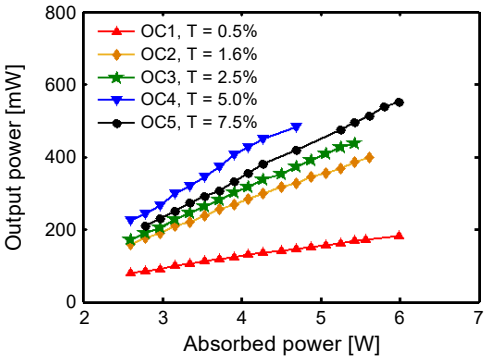

Fig. 3. Dependence of the average output power of the passively *Q*-switched Nd:LMA laser on the absorbed power for different OCs adopted.

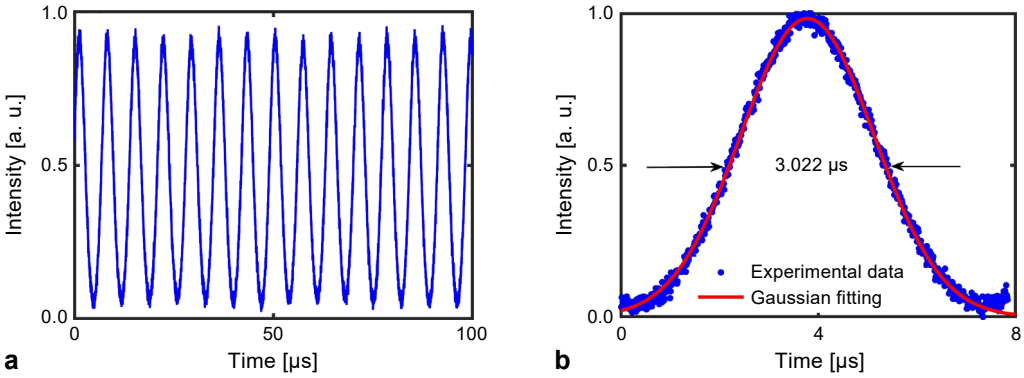

Fig. 4. Pulse trains under different scales for OC5 (T = 7.5%) under an absorbed power of 4.27 W; scale of 100 μs (**a**), and 8 μs (**b**).

an absorbed power of 5.98 W and OC5 adopted, and the corresponding light-to-light efficiency is 9.20%. However, the maximum slope efficiency of about 13.14% is obtained under OC4 utilized.

Figure 4 records the pulse trains under OC5 (T = 7.5%) adopted and an absorbed power of 4.27 W, where (**a**) and (**b**) correspond to a scale of 100 and 8 μs, respectively. From this diagram, it can be seen that the passively *Q*-switched laser is relatively stable. The single pulse is fitted by Gaussian function as shown by the red curve in Fig. 4**b**. Clearly, the output of the passively *Q*-switched laser can be regarded as a nearly Gaussian pulse. Under this case, the full width at half maximum (FWHM) of the pulse is measured to be about 3.022 μs.

Figures 5**a** and 5**b** show the pulse width and the pulse repetition frequency (PRF) as a function of the absorbed power, respectively. With the increase of the absorbed power, similar variation trends of the pulse width and the PRF are presented for different OCs adopted. The pulse widths gradually decrease while the PRFs gradually increase

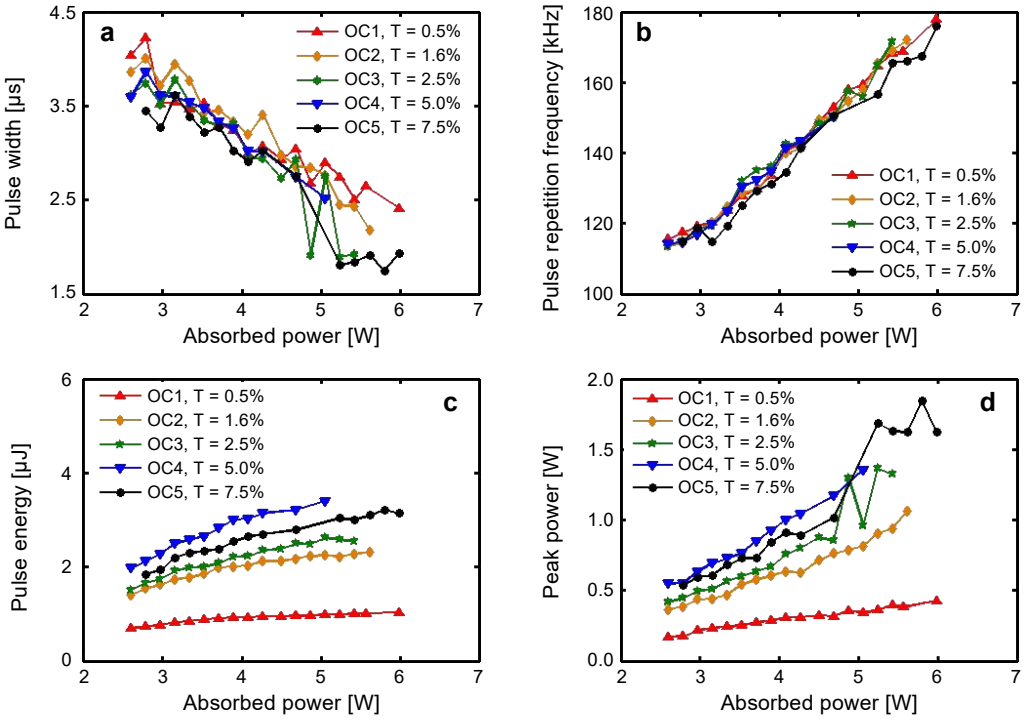

Fig. 5. Variations of the pulse width (**a**), the pulse repetition frequency (**b**), the pulse energy (**c**) and the pulse peak power (**d**) with the absorbed power.

with the increase of the absorbed power, which follows the laws of *Q*-switching [27]. The narrowest pulse width is measured to be about 1.745 μs, which is achieved under an absorbed power of 5.80 W and OC5 adopted. All PRFs are beyond 100.00 kHz, and the maximum PRF can reach 175.88 kHz under $T = 7.5\%$ and an absorbed power of 5.98 W. It is worth mentioning that the obtained pulse widths are relatively wide due to the relatively small modulation depth of SESAM (0.4%) and the relatively long cavity length of the W-type cavity (about 1 m) in this experiment. According to previously relevant reports, the modulation depth is inversely proportional to the pulse width and the cavity round trip time is directly proportional to the pulse width [28–30]. The variations of the pulse energy and peak power with the absorbed power are shown in Figs. 5**c** and 5**d**, respectively. As the absorbed power increases, the pulse energies and powers present increase trends. For a given absorbed power, the pulse energies and peak powers are different for different OCs adopted, which is easy to understand. Adopting different OC, the loss of the laser cavity is different due to different transmittance provided by the OC. As is well-known, the loss of the cavity is a key factor to determine the output characteristics of a laser. During this experiment, the maximum pulse energies for OC1–OC5 are about 1.03, 2.31, 2.54, 3.21, and 3.21 μJ, respectively, and the maximum peak powers are 0.43, 1.06, 1.32, 1.17, and 1.84 W, respectively.

4. Conclusion

In summary, through introducing a semiconductor saturable absorber mirror (SESAM) as the passively *Q*-switched device, we experimentally demonstrate a diode-pumped high-repetition-frequency (>100.00 kHz) passively *Q*-switched Nd:LaMgAl$_{11}$O$_{19}$ (Nd:LMA) laser. The output characteristics of the lasers are analyzed for adopting five mirrors with different transmittances as the output couplers (OCs). The transmittances of OC1–OC5 are 0.5%, 1.6%, 2.5%, 5.0% and 7.5%, respectively. Under continuous -wave (CW) operation, adopting a relatively high transmittance OC is favorable for achieving high output power, slope efficiency and light-to-light efficiency. Under the case of OC5 adopted, the maximum output power of 1160 mW is obtained when the absorbed power is 6.17 W, and the corresponding slope efficiency and light-to-light efficiency are 20.71% and 18.78%, respectively. After introducing a SESAM into the laser cavity, the laser can operate at a passively *Q*-switched state. When OC4 with $T = 5.0\%$ is adopted, the slope efficiency reaches the maximum value of 13.14%. For different OCs adopted, the dependences of the output performances on the absorbed power are similar. With the increase of the absorbed power, the pulse repetition frequencies (PRFs), pulse energies and peak powers increase, but the pulse widths decrease. During this work, the observed narrowest pulse width, the maximum PRF, the highest pulse energy, and the highest peak power are 1.745 μs, 175.88 kHz, 3.21 μJ, and 1.84 W, respectively.

Acknowledgements – This work was supported by the National Natural Science Foundation of China (61575163, 61775184, 61805205, and 61875167), the China Postdoctoral Science Foundation (2018M633303), the Chongqing Special Postdoctoral Science Foundation (XmT2018044), and the Fundamental Research Funds for the Central Universities (XDJK2018C079).

References

[1] Yang K.J., Zhao S.Z., Li G.G., Zhao H.M., *A new model of laser-diode end-pumped actively Q-switched intracavity frequency doubling laser*, IEEE Journal of Quantum Electronics **40**(9), 2004, pp. 1252–1257, DOI: 10.1109/JQE.2004.833227.

[2] Goel A., *Clinical applications of Q-switched NdYAG laser*, Indian Journal of Dermatology, Venereology and Leprology **74**(6), 2008, pp. 682–686, DOI: 10.4103/0378-6323.45135.

[3] Shi W., Kerr S., Utkin I., Ranasinghesagara J., Pan L., Godwal Y., Zemp R., Fedosejevs R., *Optical resolution photoacoustic microscopy using novel high-repetition-rate passively Q-switched microchip and fiber lasers*, Journal of Biomedical Optics **15**(5), 2010, article 056017, DOI: 10.1117/1.3502661.

[4] Udem T., Holzwarth R., Hänsch T.W., *Optical frequency metrology*, Nature **416**(6877), 2002, pp. 233–237, DOI: 10.1038/416233a.

[5] Marczak J., Kusinski J., Major R., Rycyk A., Sarzynski A., Strzelec M., Czyz K., *Laser interference patterning of diamond-like carbon layers for directed migration and growth of smooth muscle cell depositions*, Optica Applicata **44**(4), 2014, pp. 575–586, DOI: 10.5277/oa140408.

[6] Tian K., Yang J.N., Yi H.Y., Dou X.D., Ma Y.J., Li Y.H., Han W.J., Liu J.H., *High-power Yb:YCa$_4$O(BO$_3$)$_3$ laser passively Q-switched by a few-layer WS$_2$ saturable absorber*, Optics & Laser Technology **113**, 2019, pp. 1–5, DOI: 10.1016/j.optlastec.2018.12.001.

[7] Wang J.L., Li S., Xing Y.P., Chen L., Wei Z.Y., Wang Y.G., *A high-energy passively Q-switched Yb-doped fiber laser based on WS_2 and Bi_2Te_3 saturable absorbers*, Journal of Optics **19**(9), 2017, article 095506, DOI: 10.1088/2040-8986/aa7f5f.

[8] Keller U., Weingarten K.J., Kärtner F.X., Kopf D., Braun B., Jung I.D., Fluck R., Honninger C., Matuschek N., Aus der Au J., *Semiconductor saturable absorber mirrors (SESAM's) for femtosecond to nanosecond pulse generation in solid-state lasers*, IEEE Journal of Selected Topics in Quantum Electronics **2**(3), 1996, pp. 435–453, DOI: 10.1109/2944.571743.

[9] Keller U., *Ultrafast solid-state laser oscillators: a success story for the last 20 years with no end in sight*, Applied Physics B **100**(1), 2010, pp. 15–28, DOI: 10.1007/s00340-010-4045-3.

[10] Ren X.J., Shen D.Y., Zhang J., Tang D.Y., *Passive Q-switching of ~2.7 μm Er:Lu_2O_3 ceramic laser with a semiconductor saturable absorber mirror*, Japanese Journal of Applied Physics **57**(2), 2018, article 022701, DOI: 10.7567/JJAP.57.022701.

[11] He Y., Ma Y.F., Li J., Li X.D., Yan R.P., Gao J., Yu X., Sun R., Pan Y.B., *Continuous-wave and passively Q-switched 1.06 μm ceramic Nd:YAG laser*, Optics & Laser Technology **81**, 2016, pp. 46–49, DOI: 10.1016/j.optlastec.2016.01.027.

[12] Hao Q.Q., Pang S.Y., Liu J., Su L.B., *Tunable and passively Q-switched laser operation of Nd,Lu:CaF_2 disordered crystal*, Applied Optics **57**(22), 2018, pp. 6491–6495, DOI: 10.1364/AO.57.006491.

[13] Guan X.F., Zhan L.J., Zhu Z.W., Xu B., Xu H.Y., Cai Z.P., Cai W.W., Xu X.D., Zhang J., Xu J., *Continuous-wave and chemical vapor deposition graphene-based passively Q-switched Er:Y_2O_3 ceramic lasers at 2.7 μm*, Applied Optics **57**(3), 2018, pp. 371–376, DOI: 10.1364/AO.57.000371.

[14] Dou X.D., Ma Y.J., Zhu M., Xu H.H., Zhong D.G., Teng B., Liu J., *Multi-watt sub-30 ns passively Q-switched Yb:$LuPO_4$/WS_2 miniature laser operating under high output couplings*, Optics Letters **43**(15), 2018, pp. 3666–3669, DOI: 10.1364/OL.43.003666.

[15] Wang Y.G., Ma X.Y., Wang C.L., Lin T., Zhen K., Wang J., Zhong L., Jia Y.L., Wei Z.Y., *GaAs absorber grown at low temperature used in passively Q-switched diode pumped solid state laser*, Optica Applicata **36**(1), 2006, pp. 23–28.

[16] Koromyslov A.L., Tupitsyn I.M., Cheshev E.A., *Dual-wavelength Q-switched laser based on a lens-shaped Nd:YAG active element and a Cr^{4+}:YAG passive Q-switch*, Quantum Electronics **49**(2), 2019, pp. 95–97, DOI: 10.1070/QEL16816.

[17] Zhang H.J., Meng X.L., Liu J.H., Zhu L., Wang C.Q., Shao Z.S., Wang J.Y., Liu Y.G., *Growth of lowly Nd doped $GdVO_4$ single crystal and its laser properties*, Journal of Crystal Growth **216**(1–4), 2000, pp. 367–371, DOI: 10.1016/S0022-0248(00)00438-3.

[18] Tian Q.Y., Xu B., Zhang Y.S., Xu H.Y., Cai Z.P., Xu X.D., *1.83-μm high-power and high-energy light source based on 885-nm in-band diode-pumped Nd:YAG bulk laser operating on $^4F_{3/2} \rightarrow {}^4I_{15/2}$ transition*, Optics Express **27**(9), 2019, pp. 12565–12571, DOI: 10.1364/OE.27.012565.

[19] Di J.Q., Xu X.D., Meng J.Q., Li D.Z., Zhou D.H., Wu F., Xu J., *Diode-pumped continuous wave and Q-switched operation of Nd:LuAG crystal*, Laser Physics **21**(5), 2011, pp. 844–846, DOI: 10.1134/S1054660X11090039.

[20] Cheng M.Y., Wang Z.H., Cao Y.F., Meng X.H., Zhu J.F., Wang J.L., Wei Z.Y., *High power diode-pumped passively mode-locked Nd:YVO_4 laser at repetition rate of 3.2 GHz*, Chinese Physics B **28**(5), 2019, article 054205, DOI: 10.1088/1674-1056/28/5/054205.

[21] Schearer L., Leduc M., Vivien D., Lejus A.-M., Thery J., *LNA: a new CW Nd laser tunable around 1.05 and 1.08 μm*, IEEE Journal of Quantum Electronics **22**(5), 1986, pp. 713–717, DOI: 10.1109/JQE.1986.1073024.

[22] Pan Y.X., Zhou S.D., Wang J.W., Xu B., Liu J., Song Q.S., Xu J., Li D.Z., Liu P., Xu X.D., Xu J., *Growth, spectral properties, and diode-pumped laser operation of a Nd^{3+}-doped $LaMgAl_{11}O_{19}$ crystal*, Applied Optics **57**(32), 2018, pp. 9657–9661, DOI: 10.1364/AO.57.009657.

[23] Zhang X.Z., He J., Tang T.H., Teng B., Zhong D.G., Xu X.G., Wang Z.P., *Efficient laser operations of unprocessed thin plate of Nd:YPO_4 crystal*, Optics Express **26**(20), 2018, pp. 26179–26187, DOI: 10.1364/OE.26.026179.

[24] Czeranowsky C., Schmidt M., Heumann E., Huber G., Kutovoi S., Zavartsev Y., *Continuous wave diode pumped intracavity doubled Nd:$GdVO_4$ laser with 840 mW output power at 456 nm*, Optics Communications **205**(4–6), 2002, pp. 361–365, DOI: 10.1016/S0030-4018(02)01298-1.

[25] Lu J., Huang Z.M., Jin Z.H., Wang Y.J., Zhou F.Z., Zhang X.R., Wu G.Z., Sheng L., *Diode-pumped monolithic Nd:LMA laser*, Chinese Journal of Lasers B **3**(1), 1994, pp. 5–9.

[26] Wang J.W., Zhang Y.H., Guan X.F., Xu B., Xu H.Y., Cai Z.P., Pan Y.X., Liu J., Xu X.D., Xu J., *High-efficiency diode-pumped continuous-wave and passively Q-switched c-cut Nd:$LaMgAl_{11}O_{19}$ (Nd:LMA) lasers*, Optical Materials **86**, 2018, pp. 512–516, DOI: 10.1016/j.optmat.2018.10.053.

[27] Degnan J.J., *Theory of the optimally coupled Q-switched laser*, IEEE Journal of Quantum Electronics **25**(2), 1989, pp. 214–220, DOI: 10.1109/3.16265.

[28] Braun B., Kärtner F.X., Zhang G., Moser M., Keller U., *56-ps passively Q-switched diode-pumped microchip laser*, Optics Letters **22**(6), 1997, pp. 381–383, DOI: 10.1364/OL.22.000381.

[29] Mateos X., Loiko P., Lamrini S., Scholle K., Fuhrberg P., Suomalainen S., Härkönen A., Guina M., Vatnik S., Vedin I., Aguiló M., Díaz F., Wang Y.C., Griebner U., Petrov V., *Ho:$KY(WO_4)_2$ thin-disk laser passively Q-switched by a GaSb-based SESAM*, Optics Express **26**(7), 2018, pp. 9011–9016, DOI: 10.1364/OE.26.009011.

[30] Li J.F., Luo H.Y., Wang L.L., Zhao C.J., Zhang H., Li H.P., Liu Y., *3-μm mid-infrared pulse generation using topological insulator as the saturable absorber*, Optics Letters **40**(15), 2015, pp. 3659–3662, DOI: 10.1364/OL.40.003659.

Received April 4, 2019
in revised form September 6, 2019